

SIMULATING MARS BOUNDARY LAYER CLOUDS AND PRECIPITATION OBSERVED BY THE LIDAR ON PHOENIX.

F. Daerden, Belgian Institute for Space Aeronomy, Brussels, Belgium (Frank.Daerden@aeronomie.be), **J. A. Whiteway**, Department of Earth and Space Science and Engineering, York University, Toronto, Ontario, Canada.

Introduction:

The LIDAR instrument on the Phoenix mission uniquely observed water ice clouds that form and precipitate within the nighttime residual Planetary Boundary Layer (PBL) on Mars [Whiteway et al., 2008, 2009; Dickinson et al. 2010]. We apply a microphysical model for Mars dust and ice clouds driven by a model of the planetary boundary layer (PBL) for the interpretation of these measurements [Daerden et al. 2010]. This combined model approach simulates nighttime clouds and fall streaks within the PBL that are similar in structure to the LIDAR observations. The precipitating ice crystals are predicted to be very large (30–50 mm effective radius), resulting in downward transport of water vapor within the PBL. In combination with strong daytime mixing this process forms a local closed water cycle which acts to confine water vapor within the PBL.

Phoenix measurements of clouds and precipitation:

The Phoenix LIDAR was unique in its ability to resolve internal cloud structure and precipitation fall streaks (Figure 1). The length of the fall streaks indicated that the ice crystals had fall speeds that are consistent with prolate ellipsoids with volume-equivalent radii of ~35 mm [Whiteway et al., 2009]. The crystals would then be similar to what is found in cirrus clouds on Earth in the same temperature range, for example hexagonal columns of length 150 microns and width 50 microns [e.g., Whiteway et al. 2004].

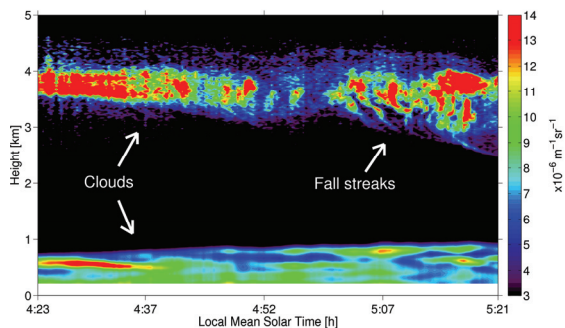


Figure 1: Contour plot of backscatter coefficient derived from the LIDAR backscatter signal at wavelength 532 nm on Phoenix sol 99 ($L_s = 122^\circ$).

Microphysical model:

A well validated microphysical model for polar stratospheric and cirrus clouds on Earth [Larsen, 2000; Larsen et al., 2002, 2004; Daerden et al., 2007] has been modified for Mars dust and water ice clouds. The model describes nucleation of water ice on dust particles and condensation and evaporation of water vapor onto and from ice particles. Dust and water ice particles are described by size-binned distributions of their number densities and ice water content. In the present study 100 size bins are used, geometrically increasing from 10 nm to 1 mm. The ice particles are assumed nonspherical with an aspect ratio of 3. After formation by heterogeneous nucleation, ice particles grow and shrink through deposition and sublimation following the basic vapor diffusion equation, applying a full kinetic approach and taking into account the Kelvin effect, exchange of latent heat, ventilation effects for diffusion and heat transfer, and effects from the nonsphericity of the particles. The detailed microphysical box model is integrated in a 1D model including explicit (size- and shape dependent) sedimentation and eddy diffusion.

Optical calculations:

For direct comparison with the LIDAR measurements the optical properties of the modeled dust and ice are calculated in the model at 532 nm. The backscatter coefficient and optical extinction are calculated using the extended precision T-matrix method for randomly oriented nonspherical particles [Mishchenko and Travis, 1998].

PBL model:

The microphysical model is driven by the temperatures and vertical eddy diffusion coefficients calculated independently by the coupled PBL-Aeolian dust model of Davy et al. [2009a] for the Phoenix lander site ($\text{lat} = 68.2^\circ$, $\text{lon} = 234.2^\circ$) at solar longitude $L_s = 122^\circ$ (Phoenix mission sol 99), which are constrained by the Phoenix air temperature measurements at a height of 2 meters above the surface [Davy et al., 2009b], see Figure 2a. The microphysical model is run on the same grid and domain as the PBL model, 241 levels over 30 km with a log-linear grid for good near-surface resolution. The initial size distribution of dust in the microphysical model is a gamma distribution with $r_{eff} = 1.6$

mm and $n_{eff} = 0.2$. The dust is distributed evenly within the PBL as indicated by the LIDAR observations.

Estimating the water profile:

The volume mixing ratio of water vapor throughout the residual boundary layer prior to cloud formation was estimated at 0.0013, distributed uniformly with height [Whiteway et al. 2009]. Near the surface the TECP instrument on Phoenix measured a diurnal cycle in water vapor ranging from 2 Pa during the day to less than 0.1 Pa in the early morning, or 0.0027 to 0.00013 in volume mixing ratio [Zent et al., 2010]. Therefore a transition zone of 1 km above the surface was assumed in which the water vapor volume mixing ratio decreases linearly with altitude from 0.0027 to the uniformly mixed part of the PBL. The resulting water column amount in the PBL is 38 pr-mm, a value consistent with space-based data [Tamppari et al. 2010].

Cloud Simulations:

The model simulation produced a cloud layer near the surface and a cloud near the PBL top (Figure 2b). The surface cloud formed at 10 p.m. and lasted until 6 a.m. At 5 a.m. it reached a maximal height of 900 m, consistent with the LIDAR observations (Figure 1). The PBL top cloud formed at 1 a.m., lasted through the early morning, and dissipated before local noon. The bulk of the cloud was located between 3.5 and 4 km, also consistent with the LIDAR observations. From the top cloud a layer of enhanced number density and backscatter coefficient is descending, which can be characterized as a fall streak. This fall streak formed at 1 a.m. and reached down to height 2.5 km at 5 a.m. similar to the observed fall streaks.

Figures 2c, 2d and 2e respectively show the modeled ice particle number density, ice particle effective radius, and the ice water content (IWC). Ice crystals in the fall streak have sizes of 35 ± 5 mm in effective radius and ~ 150 mm in length, consistent with the estimate of Whiteway et al. [2009]. Such ice crystal sizes have not previously been observed or predicted on Mars, but are typical for ice crystals sampled in cirrus clouds in the upper troposphere on Earth, where the temperatures and humidity are similar to the conditions in the PBL of Mars [Whiteway et al., 2004]. The cloud IWC was calculated by integrating the ice particle size spectrum (Figure 2e).

The maximal amount of condensed water above 200 m is 2 pr-mm, this corresponds to the estimate of Whiteway et al. [2009]. The microphysical model predicts an additional 4 pr-mm of water ice below 200 m of which the largest part is deposited as frost on the surface.

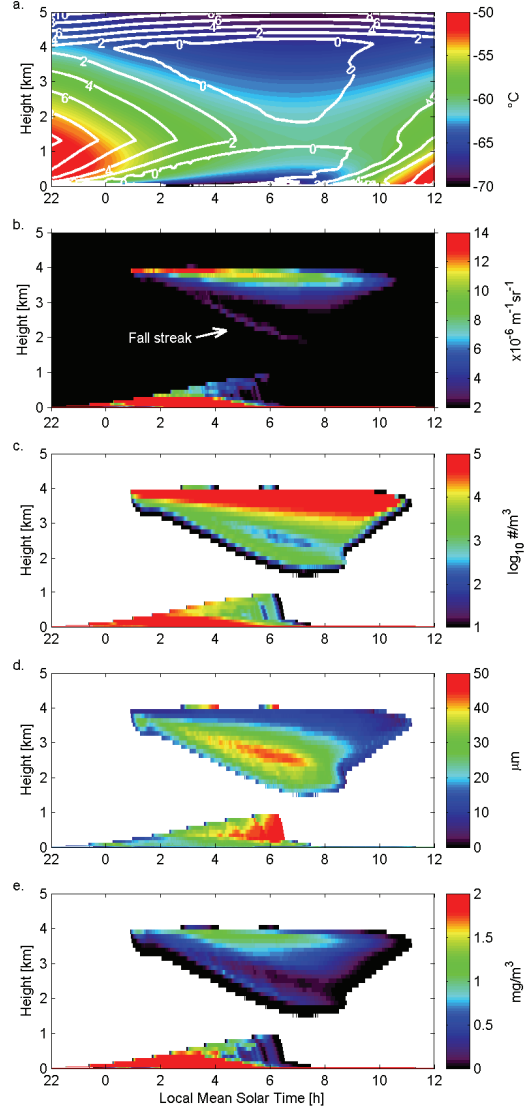


Figure 2: (a) Temperatures provided by the PBL model [Davy et al. 2009a]. Contour lines indicate elevation above frost point temperature. Model calculations: (b) Backscatter coefficient at 532 nm. (c) Ice particle number density. (d) Ice particle effective volume-equivalent radius, the length of an ice ellipsoid is $\sim 4.16 \times$ this value. (e) Cloud ice water content.

Local water cycle:

The precipitation has a considerable impact on the vertical redistribution of water vapor. At the PBL top the water volume mixing ratio decreased by more than 30%, and at 2 km (end of the fall streak) it increased by 15%.

Close to the surface the water vapor in the model remains saturated over ice throughout the night and reaches a minimum value of ~ 0.05 Pa between 1 and 4 am. This is in agreement with the measurements by

TECP on Phoenix [Zent et al., 2010]. As the sun rises, the ice crystals sublime, and the profile of humidity is mixed again over the PBL during the daytime by turbulence and convection. The water vapor profile returns to its original shape in the local afternoon.

Conclusion:

This coupled model approach demonstrated that the observations by the LIDAR on Phoenix of water ice clouds and precipitation within the PBL on Mars can be reproduced by a numerical simulation that combines models of ice microphysics, boundary layer mixing, and radiative transfer.

In this study the observed clouds at the PBL top are interpreted as indicative of a local diurnal water cycle in the PBL in which daytime mixing by convection and turbulence and nighttime cloud formation act to confine water vapor in the PBL.

References:

- Daerden, F., et al. (2007), A 3D-CTM with detailed online PSC microphysics: analysis of the Antarctic winter 2003 by comparison with satellite observations, *Atmos. Chem. Phys.*, 7, 1755-1772
- Daerden, F., et al. (2010), Simulating observed boundary layer clouds on Mars, *Geophys. Res. Lett.*, 37, L04203, doi:10.1029/2009GL041523
- Davy, R., et al. (2009a), A model of dust in the Martian lower atmosphere, *J. Geophys. Res.*, 114, D04108, doi:10.1029/2008JD010481
- Davy, R. et al. (2009b), Initial analysis of air temperature and related data from the Phoenix MET station and their use in estimating turbulent heat fluxes, *J. Geophys. Res.*, doi:10.1029/2009JE003444
- Dickinson, C., et al. (2010), Lidar measurements of clouds in the planetary boundary layer on Mars, *Geophys. Res. Lett.*, 37, L18203, doi:10.1029/2010GL044317
- Larsen, N. (2000), Polar Stratospheric Clouds. Microphysical and optical models, Scientific report 00-06, Danish Meteorological Institute
- Larsen, N. et al. (2002), Microphysical mesoscale simulations of polar stratospheric cloud formation constrained by in situ measurements of chemical and optical cloud properties, *J. Geophys. Res.*, 107(D20), 8301, doi:10.1029/2001JD000999
- Larsen, N. et al. (2004), Formation of solid particles in synoptic-scale Arctic PSCs in early winter 2002/2003, *Atmos. Chem. Phys.*, 4, 2001-2013
- Mishchenko, M.I. and Travis, L. (1998), Capabilities and limitations of a current Fortran implementation of the T-matrix method for randomly oriented, rotationally symmetric scatterers, *J. Quant. Spectrosc. Radiat. Transfer*, 60, 309-324
- Tamppari, L. K. et al. (2010), Phoenix and MRO coordinated atmospheric measurements, *J. Geophys. Res.*, 115, E00E17, doi:10.1029/2009JE003415, 2010
- Whiteway, J. et al. (2004), Anatomy of cirrus clouds: Results from the Emerald airborne campaigns, *Geophys. Res. Lett.*, 31, L24102, doi:10.1029/2004GL021201
- Whiteway, J. et al. (2008), Lidar on the Phoenix mission to Mars, *J. Geophys. Res.* 113, E00A08, doi:10.1029/2007JE003002
- Whiteway, J., et al. (2009), Mars Water Ice Clouds and Precipitation, *Science* 325, 68
- Zent, A. P. et al. (2010), Initial results from the thermal and electrical conductivity probe (TECP) on Phoenix, *J. Geophys. Res.*, 115, E00E14, doi:10.1029/2009JE003420